International Journal of Thermophysics, Vol. 15, No. 6, 1994

Efficient Evaluation of Three-Phase Coexistence Lines[1]

R. Agrawal,[2] M. Mehta,[2] and D. A. Kofke[2,3]

The Gibbs–Duhem integration method is a means for evaluating phase diagrams by molecular simulation. Starting from a state of known phase coexistence, one applies the Clapeyron equation to trace out subsequent points on the saturation line. Each simulation yields a coexistence state, and particle exchanges are not invoked to insure equality of fugacities. We describe and demonstrate here the extension of this method to three-phase coexistence, namely, among a solid, a liquid, and a gas. In one application, we compute the saturation pressure and temperature as a function of composition (more accurately, as a function of fugacity fraction) for six Lennard–Jones two-component mixtures. In a second study, we traverse a mutation pathway; that is, we evaluate three-phase equilibria *as a function of the intermolecular potential*. In particular, we define a path that transforms the Lennard–Jones model into a square well, and thus in our calculations we quantify the effect of the shape of the repulsive and attractive portions of the potential on the triple point. In the end we have what is, to our knowledge, the first estimate of a state of solid–fluid coexistence for a square-well model. In both applications we assume that the fcc crystal structure represents the thermodynamically stable solid phase.

KEY WORDS: Lennard–Jones; molecular simulation; phase equilibria; square well; triple point.

1. INTRODUCTION

The Gibbs-ensemble simulation method [1–3] has ignited an explosion of interest in the molecular simulation of phase equilibria in the past half-decade. Panagiotopoulos recently reviewed the state of affairs in this area [4], but already his report is out of date. Significant advances have since

[1] Paper presented at the Twelfth Symposium on Thermophysical Properties, June 19–24, 1994, Boulder, Colorado, U.S.A.

[2] Department of Chemical Engineering, State University of New York at Buffalo, Buffalo, New York 14260-4200, U.S.A.

[3] To whom correspondence should be addressed.

0195-928X/94/1100-1073$07.00/0

been made particularly in applying the method to chain molecules [5–8]. Despite an impressive pride of achievements, the Gibbs-ensemble method is limited by the need to perform particle exchanges which equate chemical potentials. This step makes the simulation of molecular systems quite difficult, and it so far has precluded application of the method to solid–fluid equilibria.

We recently introduced an alternative to the Gibbs-ensemble approach [9, 10]. This method—termed Gibbs–Duhem integration—relies on thermodynamic integration to evaluate and equate chemical potentials in coexisting phases. Beginning from a given coexistence state point, the method traces out a line of coexistence by integrating the Clapeyron equation. This formula is a first-order differential equation for the saturation line, and we have shown that it may be integrated using standard predictor-corrector formulas; the wrinkle in our approach is that the "integrand" is evaluated by molecular simulation. While the method is incapable of giving directly an arbitrary coexistence point, it is particularly well suited for evaluating entire phase diagrams. Gibbs–Duhem integration is appealing because it is both efficient and robust: Each simulation yields a coexistence datum, yet particle insertion is never invoked to ensure chemical potential equality.

In this report we demonstrate that the Gibbs–Duhem integration technique can be used to evaluate equilibria with crystalline phases. As an added element of interest and novelty, we focus on triple points, states of three-phase coexistence. For simple materials, this state–like the critical point—is significant because it provides a unique point of reference on the phase diagram; also, it is the lowest temperature to which the liquid can be cooled without freezing. Perhaps more important is the obvious fact that the triple point indeed lies on three coexistence lines, and thus it provides a subsequent point of departure for any of three Gibbs–Duhem integration series.

One cannot of course examine a line of triple points without adding a degree of freedom to the system—three-phase coexistence of a pure substance occurs at a unique temperature and pressure, the triple *point*. There are several ways to construct triple *lines*. The most obvious is to vary the composition. We do this in Section 2, and then in Section 3 we turn to what is perhaps a more interesting possibility, a triple line that follows a mutation pathway.

2. MIXTURES

In a recent work [11], we described two approaches for extending the Gibbs–Duhem integration method to mixtures. Both methods involve

integrating along a path in which the composition changes, but they differ in the choice of integration variable and, thus, in the independent variables selected in the series simulations. In the *semigrand* method, integration proceeds along the fugacity fraction axis, while in the *osmotic* method, the independent variable is the chemical potential of *one* of the species. Our discussion here employs an extension of the semigrand approach.

The fugacity fraction of species 2 in a binary mixture is defined as

$$\xi_2 = \frac{f_2}{f_1 + f_2} \tag{1}$$

where f_i is the fugacity of component i. With the fugacity fraction as an independent variable, the composition is not specified explicitly, and it must be determined by an ensemble average. As ξ_2 varies from zero to unity, the mixture becomes progressively rich in species 2. Simulations in this semigrand ensemble must include moves in which the molecules sample species identities, as well as spatial configurations. The Gibbs–Duhem equation written in this ensemble takes the form [11]

$$d\ln(f_1 + f_2) = h_r\, d\beta + Z d\ln p - \frac{x_2 - \xi_2}{\xi_2(1-\xi_2)}\, d\xi_2 \tag{2}$$

where h_r is the enthalpy above the ideal-gas value, p is the pressure, and $\beta = 1/k_B T$ is the reciprocal temperature, with k_B Boltzmann's constant; x_2 is the mole fraction of species 2, and $Z = \beta p/\rho$ is the compressibility factor, with ρ the number density. In deriving the Clapeyron equations for the triple-point line, we consider how β and p must vary simultaneously with ξ_2 to make the left-hand side of Eq. (2) the same when written for three coexisting phases. The result is

$$\begin{aligned} \frac{\partial \ln p}{\partial \xi_2} &= -\frac{1}{\xi_2(1-\xi_2)} \frac{H^{sl}x^g + H^{lg}x^s + H^{gs}x^l}{Z^{sl}h^g + Z^{lg}h^s + Z^{gs}h^l} \\ \frac{\partial \beta}{\partial \xi_2} &= \frac{1}{\xi_2(1-\xi_2)} \frac{Z^{sl}x^g + Z^{lg}x^s + Z^{gs}x^l}{Z^{sl}h^g + Z^{lg}h^s + Z^{gs}h^l} \end{aligned} \tag{3}$$

where $H^{\alpha\gamma} = h^\alpha - h^\gamma$, $Z^{\alpha\gamma} = Z^\alpha - Z^\gamma$, and the superscript refers to the solid (s), liquid (l), or gas (g) phase.

We performed triple-line Gibbs–Duhem series for six Lennard–Jones mixtures using the formulas above. The model parameters are summarized in Table I. The triple point of the pure Lennard–Jones substance was used to start each series; the values we adopted for this purpose were [10, 12] $kT/\varepsilon = 0.68$, $p\sigma^3/\varepsilon = 0.00106$. Subsequent points along the triple line were

determined as follows. The fugacity fraction was advanced by an increment of 0.05, and the corresponding mixture triple point was estimated by applying a "predictor" formula to each of the relations given in Eq. (3) [11]. NpT-ensemble simulations were then simultaneously initiated for each of the three coexisting phases—each simulated phase is given its own simulation volume, and thus is not in direct physical contact with the others. Averages were estimated for the enthalpy and the volume of each phase, and these quantities were used to evaluate the right-hand sides of the relations given in Eq. (3). The results were applied with a "corrector" formula to improve the estimate of the triple-point pressure and temperature. The simulation continued at the new state conditions, and the process of averaging and correcting was iterated to refine further the triple-point measurement. At the completion of the run, the fugacity fraction was again incremented and the process repeated. This continued until the state of pure species 2 was reached, corresponding to a species 2 fugacity fraction of unity. As this is once again the pure Lennard–Jones fluid, the resulting estimate for the triple-point pressure and temperature could be verified by comparison to the known values. Special measures need to be taken to evaluate the right-hand side of the relations given in Eq. (3) for the respective pure components. In these limiting cases, these quantities may be given in terms of the Henry's constants of each component in the other. Details have been presented elsewhere [11], although in the context of two-phase coexistence.

Our simulations were conducted with 108 particles in each phase. We sampled 25,000 cycles beyond an equilibration phase that sampled 5000 cycles. Here a cycle represents either one attempted translation per particle, one attempted identity change per particle, or one attempted volume change for either of the phases. The usual cubic periodic boundary conditions with the minimum-image convention were employed [13], and

Table I. Potential Parameters for the Six Mixtures Studied in Section 2[a]

Mixture	σ_{22}/σ_{11}	$\varepsilon_{12}/\varepsilon_{11}$	$\varepsilon_{22}/\varepsilon_{11}$
1	0.90	1.0	1.0
2	0.93	1.0	1.0
3	0.95	1.0	1.0
4	1.0	0.95	1.0
5	1.0	$\sqrt{0.95}$	0.95
6	0.95	0.95	1.0

[a] In all cases, $\sigma_{12} = (\sigma_{11} + \sigma_{22})/2$.

the long-range correction to the potential was considered in deciding acceptance of volume and identity changes. After every 25 cycles the current values of the simulation averages (with the long-range correction applied) were used in the corrector formula to update the imposed pressure and temperature. Stochastic errors in the averages were determined by examining 25-cycle subaverages, applying the method of Kolafa [14]; the use of longer subaverage periods had little effect on the error estimate. Errors in the triple-point temperature and pressure are more difficult to estimate. We provide error estimates for our results based on the stochastic simulation errors in the enthalpy, volumes and mole fraction, appropriately propagated to T and p with standard propagation-of-error methods [15] applied to the corrector formula. This analysis therefore ignores possible errors arising from the finite step used to integrate the relations in Eq. (3); it also discounts stability considerations, which are concerned with how errors in T and p are amplified or attenuated as the series proceeds [11].

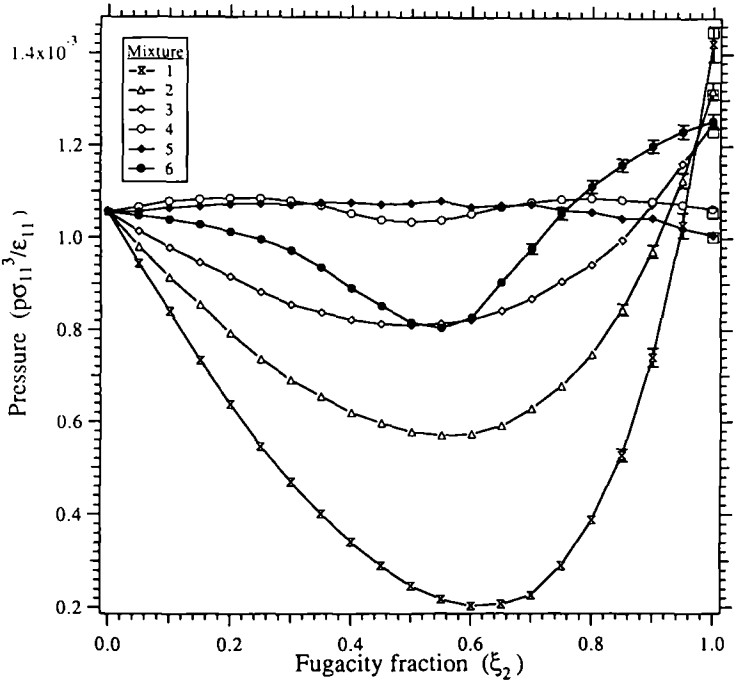

Fig. 1. Triple-point pressure of six Lennard–Jones mixtures, as a function of the fugacity fraction of species 2. Mixtures are labeled 1 to 6 in accordance with Table I. Uncertainties propagated from the stochastic errors in the simulation averages are indicated where they are larger than the plotting symbols.

An fcc symmetry was imposed on the initial configuration of the solid phase, and this persisted throughout all simulations; we did not investigate the possibility of a polymorphic transition.

Our results are presented in Figs. 1 and 2. We note first that very good agreement is seen with the pure species 2 triple points at the end of each series. A most obvious feature of the plots is the prominent influence of the size parameter. There is a deep minimum in the temperature (maximum in $1/T$) as a function of composition. This result is consistent with observations in fluid-solid (two-phase) equilibria of hard-sphere systems, in which a temperature minimum was found for size ratios less than about 0.93 [16, 17]. The hard-sphere studies further suggest the possibility of a solid-phase miscibility gap arising as the size ratio decreases below 0.9. Such a circumstance is also possible here, but we did not look for such a phenomenon. One should of course not attempt to base conclusions about

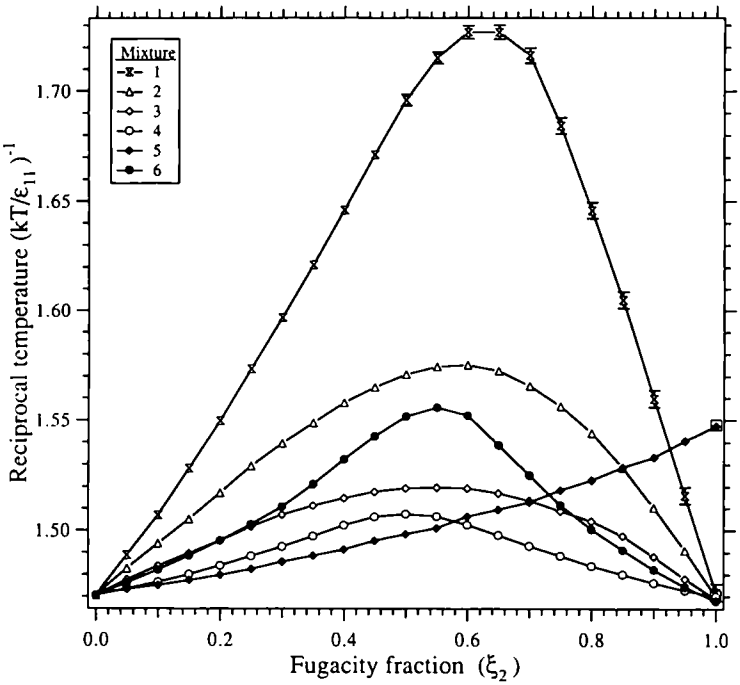

Fig. 2. Triple-point pressure of six Lennard–Jones mixtures, as a function of the fugacity fraction of species 2. Mixtures are labeled 1 to 6 in accordance with Table I. Uncertainties propagated from the stochastic errors in the simulation averages are indicated where they are larger than the plotting symbols.

the present system on results for hard spheres. Turning briefly to the other mixtures, we examined rather small deviations from unity in the energy-parameter ratios, and the effect on the triple point is of a corresponding (small) magnitude.

3. MUTATION

A mutation path is characterized by a parameter that defines the intermolecular potential. This contrasts with the familiar thermodynamic pathways, which are given as in Section 2 in terms of state parameters such as the pressure and the temperature. Mutation paths will no doubt prove very important in establishing the usefulness of the Gibbs–Duhem integration technique. A Gibbs–Duhem survey of the coexistence diagram for a given model potential cannot be taken without being first given a point on the diagram. Mutation paths present us with a very convenient means for obtaining this datum, *viz.*, integration from a coexistence point of another, better-studied, model potential (e.g., that of Lennard-Jones).

We wish to demonstrate the notion of a mutation pathway and, at the same time, show once more how Gibbs–Duhem integration is extended to study three phase coexistence. The path we shall traverse takes the Lennard–Jones (LJ) into a square-well (SW) model, and it comprises two parts, reflected by a "softness" parameter s and a "well-parameter" k,

$$u(r; s, k) = 4\varepsilon \left(\frac{\sigma}{r}\right)^{1/s} - \left[(1-k)\,4\varepsilon \left(\frac{\sigma}{r}\right)^{6} + k\varepsilon(1 - H(r - \lambda\sigma))\right] \tag{4}$$

As the parameter s decreases toward zero from the LJ value of 1/12, the repulsive part of the potential becomes increasingly hard. The parameter k is zero for the LJ model. Once we reach the limit $s = 0$, we turn the path in a direction of increasing k, reaching the SW potential at $k = 1$. In Eq. (4), $H(x)$ represents the Heaviside step function, and its application here contributes a uniform well to the potential from the hard-sphere diameter σ to a range $\lambda\sigma$; we choose λ henceforth to be 1.5.

If we treat the potential parameters s and k as independent field variables describing the state of a hybrid system, then changes in T, P, s, and k must satisfy a generalized Gibbs–Duhem equation

$$d \ln f = h\, d\beta + Z d \ln p + \Lambda_s\, ds + \Lambda_k\, dk \tag{5}$$

This formula defines A_s and A_k, each of which may in turn be expressed in the form of an NpT ensemble average,

$$A_s = -\frac{4\beta\varepsilon}{s^2}\left\langle\left(\frac{\sigma}{r}\right)^{1-s}\ln(\sigma/r)\right\rangle_{NpT}$$
$$A_k = \beta\varepsilon\left\langle 4\left(\frac{\sigma}{r}\right)^6 - (1 - H(r-\lambda\sigma))\right\rangle_{NpT} \tag{6}$$

Thus they may be readily computed in a molecular simulation. We proceed as before to derive Clapeyron formulas that characterize the saturation lines along s and k,

$$\frac{\partial \ln p}{\partial t} = \frac{H^{sl}A_t^g + H^{lg}A_t^s + H^{gs}A_t^l}{Z^{sl}h^g + Z^{lg}h^s + Z^{gs}h^l}$$
$$\frac{\partial\beta}{\partial t} = -\frac{Z^{sl}A_t^g + Z^{lg}A_t^s + Z^{gs}A_t^l}{Z^{sl}h^g + Z^{lg}h^s + Z^{gs}h^l} \tag{7}$$

where t is either s or k, and other quantities are as defined in the previous section.

The only difficulty encountered in the integration series occurs as the hard-core limit is approached, i.e., $s \to 0$. In this case, A_s becomes increasingly difficult to evaluate by simulation averaging according to Eq. (6). Fortunately, we can develop an alternate expression for A_s in this limit by expanding the pair distribution function about the contact value ($r = \sigma$). We may further transform the result by applying the pressure equation, which gives the pressure in terms of the radial distribution function [18]; finally, we have

$$A_s = 3[Z - 1 + 4\beta\varepsilon\langle(\sigma/r)^6\rangle][\gamma + \ln(4\beta\varepsilon)] \tag{8}$$

where γ is Euler's constant. To evaluate the compressibility factor Z, we used the predictor/corrector pressure and temperature and the simulation average of the density.

We performed a Gibbs–Duhem integration series along the triple-line path connecting the LJ and SW models. The pressure integration proceeded almost as prescribed by Eq. (7), the difference being that we applied a formulation with the pressure p itself as a dependent variable, rather than $\ln(p)$. Most details of the integration procedure follow as in the previous section. Beginning with $s = 1/12$ and $k = 0$, a step in s was taken

to $s = 0.08$, and subsequently steps of 0.01 were taken to $s = 0.01$. The final step to $s = 0$ we completed by evaluating A_s according to Eq. (8). The resulting point of coexistence was then used to begin an integration series in k, applying steps of 0.1 to take k from zero to unity.

The simulations employed 108 particles in the solid and vapor phases and 128 in the liquid. The usual cubic periodic boundaries were applied to the solid and vapor, while the liquid was simulated in a periodic truncated octahedral cell [13]. We sampled 10,000 cycles beyond relaxation phases of 10,000 or 5000 cycles for the paths in s and k, respectively; a cycle here comprises one attempted translation per particle and 10 attempted volume changes (among all phases). Subsequent to the calculations reported in

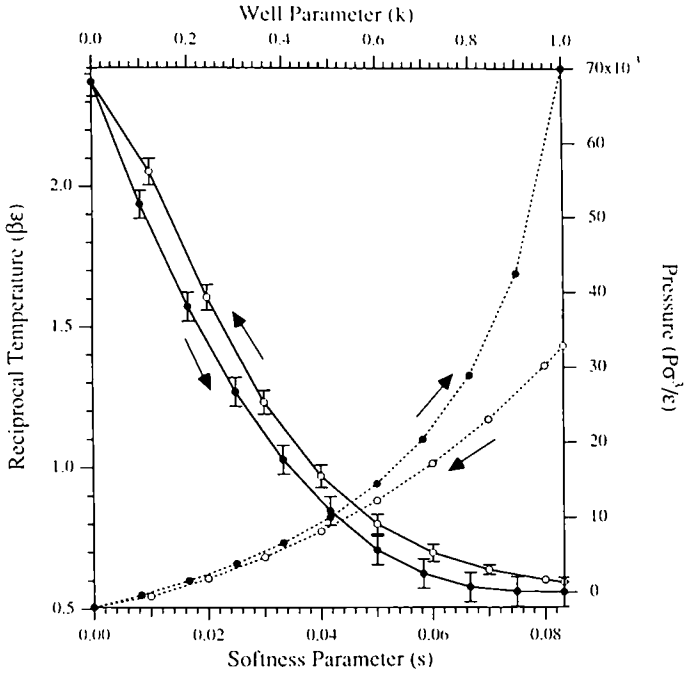

Fig. 3. Triple-point temperature (dashed lines) and pressure (solid lines) observed as the Lennard–Jones potential is mutated into the square well in the manner described by Eq. (4) (with $\lambda = 1.5$). The open circles are the s pathway (along which k is held fixed at zero), and the filled circles describe the k pathway (along which s is held fixed at zero). The procedure begins at the right and traces that path indicated by the arrows. Uncertainties propagated from the stochastic errors in the simulation averages are indicated where they are larger than the plotting symbols.

Section 2, we applied the Gibbs–Duhem integration method to compute the LJ triple point: [19] $kT/\varepsilon = 0.698$, $p\sigma^3/\varepsilon = 0.00135$; this result was used to initiate the present Gibbs–Duhem mutation series.

The saturation temperatures and pressures so computed are presented in Fig. 3. It is interesting to see that the effect of changing the attractive well is counter to that of increasing the hardness of the repulsion. The pressure curve, in particular, almost retraces itself as s and k are varied in turn. Much of this effect may be explained by the fact that the well depth increases significantly as $s \to 0$ and is restored upon the increase in k. While the triple-point temperature also retraces itself to some extent, it has nevertheless been cut almost in half by the process, settling to a value of about 0.41 for this ($\lambda = 1.5$) square-well model. The triple-point pressure varies over a rather wide scale during this process, and we feel that more accurate results may have been obtained by applying Eq. (7) as written [i.e., in terms of $\ln(p)$]; this calculation is currently under way. Also, the final step taken to $s = 0$ seems slightly out of line with the trend to $s = 0.01$, and we are more carefully examining our application of Eq. (8) to see if it has introduced additional uncertainty at this point. Pending completion of these verifications we will withold a final proclamation of our measurement of the $\lambda = 1.5$ square-well triple point.

ACKNOWLEDGMENTS

This work was supported by the National Science Foundation, under the Presidential Young Investigator program. Computing equipment used to perform these calculations was obtained with additional NSF support, under Grant CTS-9212682.

REFERENCES

1. A. Z. Panagiotopoulos, *Mol. Phys.* **61**:813 (1987).
2. A. Z. Panagiotopoulos, N. Quirke, M. Stapleton, and D. J. Tildesley, *Mol. Phys.* **63**:527 (1988).
3. B. Smit, P. de Smedt, and D. Frenkel, *Mol. Phys.* **68**:931 (1989).
4. A. Z. Panagiotopoulos, *Mol. Sim.* **9**:1 (1992).
5. M. Laso, J. J. de Pablo, and U. W. Suter, *J. Chem. Phys.* **97**:2817 (1992).
6. G. C. A. M. Mooij, D. Frenkel, and B. Smit, *J. Phys. Condens. Matter* **4**:L255 (1992).
7. J. I. Siepmann, S. Karaborni, and M. L. Klein, submitted for publication.
8. J. I. Siepmann, S. Karaborni, B. Smit, and M. L. Klein, Monte Carlo simulations of the phase behavior of alkanes and perfluorinated alkanes, presented at AIChE Spring Meeting, Atlanta, GA (1994).
9. D. A. Kofke, *Mol. Phys.* **78**:1331 (1993).
10. D. A. Kofke, *J. Chem. Phys.* **98**:4149 (1993).
11. M. Mehta and D. A. Kofke, *Chem. Eng. Sci.* **49**:2633 (1994).

12. J.-P. Hansen and L. Verlet, *Phys. Rev.* **184**:151 (1969).
13. M. P. Allen and D. J. Tildesley, *Computer Simulation of Liquids* (Clarendon Press, Oxford, 1987).
14. J. Kolafa, *Mol. Phys.* **59**:1035 (1986).
15. J. R. Taylor, *An Introduction to Error Analysis* (University Science Books, Mill Valley, 1982).
16. W. G. T. Kranendonk and D. Frenkel, *J. Phys. Condens. Matter* **1**:7735 (1989).
17. D. A. Kofke, *Mol. Sim.* 7:285 (1991).
18. D. A. McQuarrie, *Statistical Mechanics* (Harper & Row, New York, 1976).
19. R. Agrawal and D. Kofke, *Mol. Phys.* (submitted).